NMR structure of the Arctic mutation of the Alzheimer's Aβ(1–40) peptide docked to SDS micelles

ARTICLE *in* JOURNAL OF MOLECULAR STRUCTURE · NOVEMBER 2014

Impact Factor: 1.6 · DOI: 10.1016/j.molstruc.2014.08.030

Journal of Molecular Structure 1076 (2014) 518–523

Contents lists available at ScienceDirect

Journal of Molecular Structure

journal homepage: www.elsevier.com/locate/molstruc

NMR structure of the Arctic mutation of the Alzheimer's Aβ(1–40) peptide docked to SDS micelles

K.S. Usachev [a,*], A.V. Filippov [a,b], B.I. Khairutdinov [a,c], O.N. Antzutkin [b,d], V.V. Klochkov [a]

[a] Kazan Federal University, Kremlevskaya, 18, Kazan 420008, Russian Federation
[b] Chemistry of Interfaces, Luleå University of Technology, Luleå SE-97187, Sweden
[c] Kazan Institute of Biochemistry and Biophysics, Russian Academy of Sciences, P.O. Box 30, Kazan 420111, Russian Federation
[d] Department of Physics, Warwick University, CV4 7AL Coventry, UK

HIGHLIGHTS

- Solution structure of "Arctic" mutant of Aβ1–40 amyloid peptide in SDS micelles.
- Both mutant and wild-type interactions are hydrophobic in nature.
- Peptide conformation is very sensitive to single amino acid substitutions.
- Peptide-to-membrane binding is very sensitive to single amino acid substitutions.

GRAPHICAL ABSTRACT

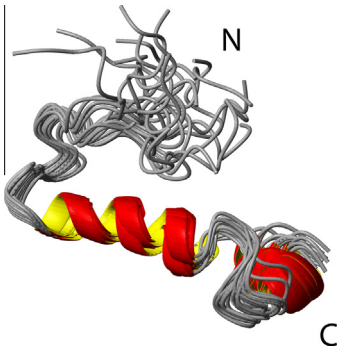

ARTICLE INFO

Article history:
Received 21 May 2014
Received in revised form 14 August 2014
Accepted 15 August 2014
Available online 22 August 2014

Keywords:
NMR
Structure
Amyloid β-peptide
"Arctic" mutation
SDS micelle

ABSTRACT

The "Arctic" point mutation of the Alzheimer's amyloid β-peptide is a rare mutation leading to an early onset of Alzheimer's disease. The peptide may interact with neuronal membranes, where it can provide its toxic effects. We used 2D NMR spectroscopy to investigate the conformation of the "Arctic" mutant of Aβ1–40 Alzheimer's amyloid peptide in sodium dodecyl sulfate micelle solutions, which are the type of amphiphilic structures mimicking some properties of biomembranes. The study showed that the Arctic mutant of Aβ1–40 interacts with the surface of SDS micelles mainly through the Leu17–Asn27 3_{10}-helical region, while the Ile31–Val40 region is buried in the hydrophobic interior of the micelle. In contrast, wild-type Aβ1–40 interacts with SDS micelles through the Lys16–Asp23 α-helical region and Gly29–Met35. Both the Arctic mutant and the wild-type Aβ1–40 peptides interactions with SDS micelles are hydrophobic in nature. Aβ peptides are thought to be capable of forming pores in biomembranes that can cause changes in neuronal and endothelial cell membrane permeability. It has also been shown that Aβ peptides containing the "Arctic" mutation are more neurotoxic and aggregate more readily than the wild-type Aβ peptides at physiological conditions. Here, we propose that the extension of the helical structure of Leu17–Asn27 and a high aliphaticity (neutrality) of the C-terminal region in the Arctic Aβ peptides are consistent with the idea that formation of ion-permeable pores by Aβ oligomers may be one of prevailing mechanisms of a larger neuronal toxicity of the Arctic Aβ compared to the wild-type Aβ peptides, independent of oxidative damage and lipid peroxidation.

* Corresponding author.
E-mail address: k.usachev@kpfu.ru (K.S. Usachev).

http://dx.doi.org/10.1016/j.molstruc.2014.08.030
0022-2860/

Introduction

Alzheimer's disease (AD) is the most common age-related dementia, which is characterized by amyloid plaque formation in the brains of AD patients. The main component of the amyloid plaque is amyloid β-peptide (Aβ peptide), which contains 39–42 amino acid residues depending on the variant. For all Aβ peptides, the lethal action is linked to a pathological conversion or "misfolding" of its native, non-toxic (globular or "natively unfolded") structure into toxic aggregates. Evidence suggests that the ability to form toxic Aβ assemblies is an intrinsic property of the protein's primary sequence, without any requirement for post-translational modification or specific enzyme activities [1–4]. As has recently been established, mature amyloid fibrils are not the most toxic forms of amyloidogenic proteins, but oligomers formed early during the aggregation process are very toxic [1,2,5,6]. Different proteins/peptides, including Alzheimer's Aβ peptides, can form toxic oligomers, all of them exhibiting a similar morphology and sensitivity to the same antibody [7]. These soluble protein oligomers seem to be the main toxic species [8]. Kayed et al. [7] suggested a potential role for cellular membranes in the neurotoxic activity of these oligomeric structures. These oligomers can bind to synaptic membranes [6], but the biochemical mechanism by which soluble oligomers associate with membranes and tamper with different signalling pathways is yet unclear [9].

The Alzheimer's amyloid peptide contains a central hydrophobic cluster (amino acid residues 17–21) that is suggested to play an important role in peptide aggregation [10–12]. A number of single-residue mutations in the Aβ peptide sequence has been reported [13,14] and studies have characterized some of the mutations in the central "16–23" cluster: the Dutch (E22Q [15]), Italian (E22K [16]), Arctic (E22G [17–19]), Flemish (A21G [20]), Iowa (D23N [21]) and Osaka (or Japanese, E22Δ [22]) mutations. These Aβ peptides have a single amino acid change or a deletion at the Aβ peptide position 21–23. The fibrillogenic properties of Aβ variants with different lengths were found to have changed in these mutants [13,18,19,22,23]. As a result, Aβ1–40 and Aβ1–42 variants containing these mutations are more neurotoxic and aggregate more readily than the wild-type (wt) peptide in *in vitro* experiments [24].

The "Arctic" (E22G) single-point mutation of the Alzheimer's Aβ peptide is a rare mutation found in a few families in northern Sweden, leading to an early onset of Alzheimer's disease (52–57 years old) [19]. This mutation is the only known intra-β-amyloid mutation to date causing the more typical clinical picture of Alzheimer's disease [25]. It has been shown that the Arctic Aβ1–40 peptide has higher rates of oligomerization and fibrillation, which occur *in vitro* at physiological conditions at lower peptide concentrations [18,19,26–28] and at lower plasma levels *in vivo* [19,29,30] compared to the wild-type Aβ1–40 peptide. Arctic Aβ1–40 fibrils exhibit a variety of distinct morphologies, significantly different from those of the wild type [28]. From the molecular point of view, the Arctic mutation replaces a polar, negatively charged glutamic acid at the position 22 with a nonpolar, neutral glycine. This also represents a change in the hydropathy index [31] from 23.5 to 20.4, increasing the hydrophobic nature of the peptide. In addition, because of the Glu −>Gly (negative charge − >neutral) mutation, pI of the Arctic Aβ1–40 shifts from ca 5.5 (for the wild-type Aβ1–40) toward more neutral pH values, thus affecting solubility of the Arctic mutant around the physiological pH (pH 7.4).

Experimental studies as well as molecular dynamics simulations on full-length wt-Aβ indicate that this peptide is mostly unstructured (random coil) in aqueous solutions but bears some regions of structural order [32–34]. Simulations reveal that when residue E22 is mutated ("E22*X*," where *X* is K, G, or Q), there is very little change in peptide structure relative to wt-Aβ. Therefore, it was believed that Aβ peptide interaction with cellular membranes is involved in AD pathogenesis and plays a central role in neurodegeneration [26,27,35–41]. However, the typical biological membrane is a complex structure composed primarily of lipids and proteins. To investigate the molecular details of peptide or protein structure by NMR, relevant models for the membrane bilayer are necessary [42]. Typical membrane models in biophysical studies of protein and peptide-lipid interactions include vesicles (or liposomes) [43–45], bicelles [46–48], and detergent micelles [47–49]. The choice of membrane mimetic is very much dependent on the methodology to be used. For solution NMR studies it is a firm prerequisite that the model membrane reorients sufficiently rapid to achieve good spectral resolution. This requisite imposes a rather strong limitation on the kinds of model membranes that are appropriate. Unfortunately, vesicles (both large and small) are not good choice, because their large size or very large surface curvature [42,49]. Therefore, a micellar membrane model is preferred. Micelles consist of detergent molecules that aggregate above a certain threshold concentration, the critical micelle concentration (CMC), while an increase in the detergent concentration to above CMC results in the formation of more micelles, rather than larger micelles [42]. Micelles are relatively small that provides their rapid thermal rotation on the time-scale required for NMR. Sodium dodecyl sulfate (SDS) micelles have been used successfully before to determine solution structure of peptides [50–53]. Synthetic SDS micelles, like several biomembranes, have a negatively charged surface. Of course, the membrane charge is not as high as the charge of SDS micelles, but the micelle ionization fraction is only 30%, therefore, electrostatics does not always interfere for non-electrostatic interactions (e.g. van der Waals) to come into play, as it has been shown before [54].

Although neurotoxicity is produced by aggregated Aβ peptide structures, the interaction of monomeric Aβ peptides with cellular membranes may serve as a basis for elucidating the aggregation mechanisms of Aβ peptides. In addition, the formation of ion-permeable pores by Aβ oligomers is thought to be a possible mechanism for neuronal toxicity, independent of oxidative damage and lipid peroxidation [55]. The binding and misfolding of these proteins on biomembrane surfaces is yet poorly understood, so to reveal the exact mechanism of aggregation of the wild-type and mutants of Aβ peptides and to determine their spatial structures in biomembrane mimicking environments is highly important. Therefore, in this paper we studied the spatial structure of the Arctic Aβ1–40 peptide monomer in an SDS-water system using multidimensional NMR spectroscopy, which is a good technique for such studies [51,56,57].

Experimental

Materials

The Arctic mutant Aβ1–40 peptide was synthesized by solid-phase peptide synthesis, using amino acids protected by the 9-fluorenylmethoxycarbonyl group and with reaction mixture conductivity control. Fmoc-protected amino acids of "peptide synthesis" grade were purchased from Applied Biosystems, Foster City, CA, USA. Peptide synthesis was done using the 0.1 mmol automated fast Fmoc solid phase procedure using HBTU (H-benzotriazole-1-yl-tetramethyluranium hexafluorophosphate) activation. The procedure was performed on an ABI 433A peptide synthesizer (Applied Biosystems) at 293 K. Cleavage from the resin and separation of the peptide substrate and the protecting groups was carried out in a solution of phenol, ethanedithiol and thioanisole in 95% trifluoroacetic acid, followed by precipitation of the peptide in cold

tert-butyl methyl ether (tBME). The peptide was purified using the high-performance liquid chromatography instrument Series 200 Perkin–Elmer HPLC System (Waltham, MA, USA). A semipreparative Vydac 259VH810 reverse phase column was used at 328 K, with a water-acetonitrile linear gradient with 0.1% trifluoroacetic acid (TFA) and flow rate of 4 mL/min. The quality of the final product was characterized using electrospray mass spectrometry. The purity of the peptide was estimated as better than 95%. The sample was lyophilized and stored at a temperature of 193 K before use.

The perdeuterated sodium dodecylsulfate (SDS, ^{2}H 98%, Aldrich) micelle solutions in $H_2O + D_2O$ (90 + 10%) and in D_2O (100%) were prepared at a concentration of 5.72 g/L, i.e. *ca* 199 mM. The Arc-Aβ1-40(E22G) peptide was dissolved in the micelle solution immediately before the NMR experiments. The peptide concentration was ~300 μM. CMC of SDS in water is approximately 8.2 mM at room temperature. Therefore, the micellar SDS solution has a concentration of *ca* 192 mM, and at the peptide concentration of 300 μM, the peptide/SDS ratio on the micelle surface is expected to be *ca* 0.00156, i.e. one peptide molecule per *ca* 636 molecules of SDS. The aggregation number of SDS at CMC is equal to 62 and an increase in the detergent concentration above CMC results in the formation of more 62-molecule size micelles, rather than micelles of a larger size. Therefore, we do not expect interaction of more than one peptide molecule with a SDS micelle. All spectra were acquired at 293 K.

All 2D NMR spectra were acquired in less than 48 h after sample preparation to minimize the amount of aggregates for the NMR experiments. 1D NMR spectra were collected before and after the 2D experiments to check peptide sample stability.

NMR spectroscopy and spatial structure calculation

All data were acquired using a 500 MHz (^{1}H) Bruker (BRUKER BIOSPIN AG, Faellanden, Switzerland) Avance II NMR spectrometer.

For each 2D NOESY and TOCSY spectrum, 32 signal transients were collected using 16 dummy scans with spectral widths of 12 ppm in both dimensions, using 2048 complex points for F2 and 1024 complex points for F1. All chemical shifts were measured from two-dimensional TOCSY spectra. The proton chemical shifts were referred to the 3-(trimethylsilyl)-propionic-2,2,3,3–$^2H_4$ acid (TMSP-2,2,3,3-$^2H_4$) (98% atom ^{2}H, Aldrich). The spin-lock time of the TOCSYs was 75 ms and 150 ms. The solvent signal was suppressed using the "3-9-19" pulse sequence with gradients. NOESY data were collected with a mixing time of 400 and 500 ms to derive ^{1}H–^{1}H distance constraints.

Spectra were processed by NMRPipe [58] and analyzed using SPARKY [59]. Sequence-specific backbone resonance assignments and side-chain assignments for all residues were obtained using a combination of 2D TOCSY and NOESY experiments.

Inter-proton distances obtained from analysis of intensities of cross-peaks from NMR NOESY spectra were used as the primary data for the calculations by the molecular dynamics method in the Xplor-NIH program [60]. Following structural calculations, the ensemble of structures was subjected to restrained molecular dynamics using the Xplor-NIH [60]. A total of 1000 structures were calculated and 20 with minimal energy were chosen in both cases. None of the 20 structures had any violated NOE distances. Individual structures were minimized, heated to 1000 K for 6000 steps, cooled in 100 K increments to 50 K, each with 3000 steps, and finally minimized with 1000 steps of the steepest descent, followed by 1000 steps of conjugate gradient minimization. Starting with a family of 1000 structures, approximately 200 were subjected to subsequent molecular dynamics calculations and, finally, the 20 lowest energy structures were retained. The most probable structure of the "peptide-micelle" complex was determined by binding the hydrophobic area of the peptide on the charged micelle surface.

The Aβ peptide structures were visualized with MOLMOL [61] and CHIMERA [62].

Results and discussion

Chemical shift assignments of Arc-Aβ1-40(E22G) in SDS micelles were produced by 2D NMR ^{1}H–^{1}H TOCSY and NOESY experiments (Table 1). Exchange rates between water and H_N protons were analyzed by detection of peaks in ^{1}H and ^{1}H–^{1}H TOCSY spectra and observed cross-peaks were treated as an indication of water-exposed amide groups.

In NOESY NMR spectra of Arc-Aβ1-40(E22G) in SDS micelles, there were numerous inter- and intra-residue cross peaks (Fig. 1). The presence of $dNN_{(i,i+1)}$, $d\alpha N_{(i,i+3)}$, and $d\alpha N_{(i,i+2)}$ medium range NOE connectivities is an indication of partially folded structure suggest that the peptide adopts a 3_{10} helix in the region comprising residues Leu17-Asn27 and a pi-helical structure within the region expanding Leu34-Gly37 (Fig. 2). A total of 488 interproton NOE distance constraints were determined for the structural calculations (see Table 2). Numerous medium-range NOE connectivities allowed us to construct the 3D structure of Arc-Aβ1-40(E22G) in SDS micelles by molecular dynamics method calculations of the Xplor-NIH program. A total of 1000 structures were calculated and 20 with minimal energy were chosen (Fig. 3).

In the SDS micelle solution with Arc-Aβ1-40(E22G), we observed two helical regions: a 3_{10}-helical region (residues 17–27) and a pi-helical region (residues 34–37). Hydrogen/deuterium exchange experiments (HDX) reveal that residues Asp7–Tyr10, Phe19, Val24–Asn27, and Val 39 show intermediate protection and residues from Ile31–Gly37 are the most protected to exchange (Fig. 2). Based on this data, we proposed that the Ile31–Val40 region is buried in the hydrophobic interior of the micelle. The most probable structure of the "peptide-micelle" complex was determined by binding the hydrophobic area of the peptide on the charged micelle surface [52,62]. The final structure of the Arc-Aβ1-40(E22G) peptide bound to an SDS micelle is presented in Fig. 4. From this figure, it is evident that Arc-Aβ1-40(E22G) interacts with SDS micelles through its Leu17-Asn27 3_{10}-helical and Ile31-Val40 regions.

We observed distinct differences between our obtained structure of the Arc-Aβ1-40(E22G) and the structure of the wild type Aβ1-40 peptide, and its fragments, in the same SDS environment and under the same conditions [51,52,62,63]. Indeed, chemical shift changes and structure calculations showed that Aβ1-40 of the wild type interacts with the surface of the SDS micelle mainly through the Lys16–Asp23 α-helical region. There have been several differing reports of NMR solution structures of Aβ peptides and their fragments under a wide variety of experimental conditions [64–71]. Aβ peptides were primarily found to form α-helical structures in SDS micelle/H_2O, trifluoroethanol/H_2O or hexafluoroisopropanol/H_2O solutions. There were two predominantly formed α-helical regions of the Aβ peptide (residues 15–23 and 28–35). Jarvet et al. [50] have observed that for the wild-type Aβ1–40 in SDS micelles, the two α-helices induced in Aβ1–40, comprising residues 15–24 and 29–35, respectively, are surrounded by flexible, unstructured regions. In contrast, the Arctic mutant of Aβ1-40 interacts through the Leu17–Asn27 3_{10}-helical region and the Ile31–Val40 region. The former part of the peptide forms a 3_{10}-helical region, which also has been observed in the Aβ11-28 fragment of the Arctic mutant peptide [70]. Moreover, the 3_{10}-helix type is very unstable and could easy convert to other unstructured or α-helical structures. Therefore, the 3_{10}-helical structure in the Arctic variant could lead to much faster aggregation than the α-helically more stable Aβ1-40 [70].

The effect of the E22G point mutation on peptide structure has been studied in a number of experimental works and simulations.

Table 1
^{1}H NMR chemical shifts of Arc-Aβ1–40(E22G) in SDS micelle solution.

Amino acid residue	^{1}H chemical shift (ppm)				
	NH	Hα	Hβ	Hγ	Others
D1		4.34	2.97, 2.95		
A2	8.51	4.35	1.30	1.71, 1.49	
E3	8.18	4.26	2.00, 1.94		
F4	7.88	4.59	3.16, 3.06		7.28 (3/5), 7.03 (2/6)
R5	7.81	4.15	1.78		7.10(δNH), 3.15, 3.08 (δ)
H6	8.16	4.68	3.34, 3.19		7.31 (4)
D7	8.30	4.67	2.89		
S8	8.24	4.39	3.89	2.71, 2.52	
G9	8.33	3.95, 3.91		0.94, 0.88	
Y10	7.90	4.44	2.96		7.07 (2/6), 6.78 (3/5)
E11	7.92	4.32	2.22, 2.14		
V12	7.88	3.99	2.03	2.35	
H13	8.32	4.70	3.18	1.63	7.34 (4)
H14	8.06	4.84	3.40, 3.16	1.69	7.48 (4)
Q15	8.54	4.07	2.09	0.96, 0.90	7.38 (ε), 6.83 (ε)
K16	8.31	4.23	1.94, 1.85		3.03 (ε), 1.71 (δ)
L17	7.63	4.28	1.87		0.95, 0.89 (δ)
V18	7.64	3.79	2.11		
F19	7.84	4.39	3.13, 3.04		7.28 (2/6), 7.04 (3/5)
F20	7.95	4.44	2.97, 2.87		7.29 (3/5), 7.05 (2/6)
A21	8.24	4.03	1.49	0.90	
G22	8.17	3.89			
D23	8.03	4.67	2.89		
V24	7.94	3.83	2.12		
G25	8.45	4.09, 3.83		1.51	
S26	8.04	4.42	3.98, 3.94		
N27	8.10	4.96	2.92, 2.74		7.62, 6.95 (γNH$_2$)
K28	7.93	4.05	1.91	1.68	7.49 (εNH), 3.04 (ε), 1.73 (δ)
G29	8.63	4.04, 3.83			
A30	7.96	4.23	1.38		
I31	8.01	3.78	2.05	1.64	0.94 (γ), 0.90 (δ)
I32	8.09	3.79	1.91	2.95	1.02 (γ), 0.95 (δ)
G33	8.09	3.89, 3.81		1.02, 0.97	
L34	7.68	4.21	1.95, 1.85		0.93 (δ)
M35	7.91	4.33	2.22, 2.16		
V36	8.14	4.05	2.23	0.99	
G37	8.00	4.04, 3.99		0.97	
G38	8.08	4.01			
V39	7.90	4.16	2.15	1.71, 1.49	
V40	7.78	4.27	2.17		

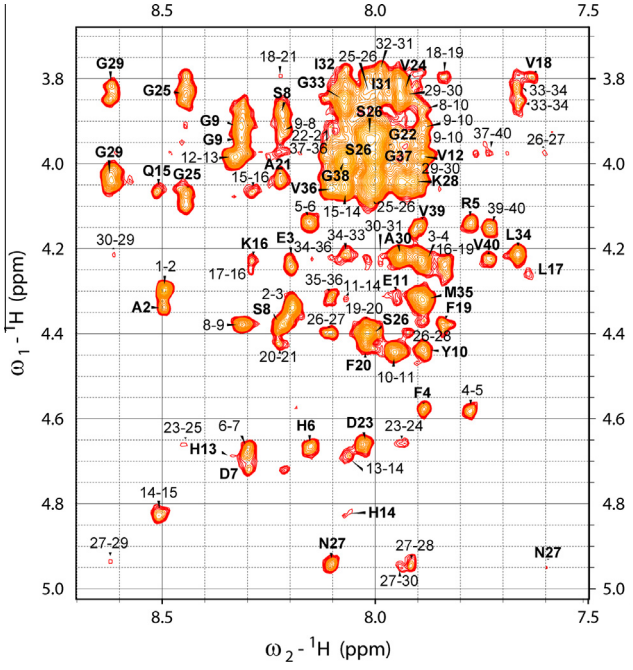

Fig. 1. Fingerprint NH-Hα region of a 2D NMR ^{1}H–^{1}H NOESY spectrum acquired at 500 MHz of Arc-Aβ1–40(E22G) in a solution of H_2O + D_2O with SDS micelles. Mixing time t_m = 0.4 s.

MD simulations of Krone et al. [72] reveal that the 24–28 bend motif is retained in all E22 mutants, suggesting that mutations involving residue E22 may not affect the structure of the folding nucleation site of Aβ peptides. Enhanced aggregation in Aβ with familial Alzheimer's disease substitutions may result from the following: (i) The depletion of the E22–K28 salt bridge may lead to further stabilization of the specific bend structures involving the D23–K28 salt bridge detected in a number of polymorphs of Aβ amyloid fibrils. (ii) The E22 mutations may affect flexibility of the peptide in the bending region near the hydrophobic L17–A21 core and/or (iii) longer-range interactions outside the 21–30 residue position that can impact the aggregation of Aβ. (iv) pI of the peptides shifts toward more neutral pH values, thus lowering solubility of the E22 mutations in aqueous solutions near the physiological pH 7.4, compared to the wild type Aβ peptides. The possible "intermediate" bend structure in wt-Aβ1-40 with the E22–K28 salt bridge must presumably rearrange itself to produce other conformations (i.e. with the D23–K28 salt bridge) capable of forming fibrils. This could lead to a slower aggregation rate for the wt-Aβ1–40 peptide compared to E22X mutants of Aβ1–40. The detailed structures of wt-Aβ1–40 and the Arctic mutant of Aβ11–28 fragments under SDS-water micelle conditions have been determined by Rodziewicz-Motowidloet al. [70] using CD, 2D NMR and molecular dynamics techniques. They showed that the Aβ11–28 peptide structure is more stable and better defined than that of Aβ11–28(E22G). Analysis showed that the side chains of the native peptide fragment embedded farthest into the micelle interior are

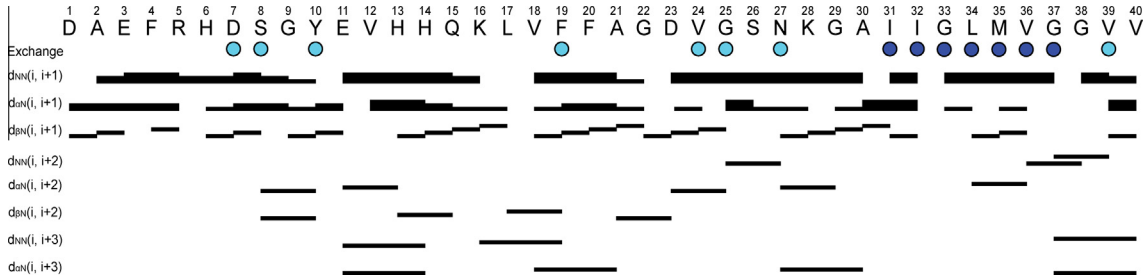

Fig. 2. Summary of the inter-residue NOE connectivity observed in the 2D NOESY spectra for the Arc-Aβ1–40(E22G) peptide embedded into SDS micelles. The line thickness for the NOE connectivity is inversely proportional to the squared upper distance bound. The NOE information on some regions was restricted due to cross-peak broadening and overlapping. Residues with a slowly exchanging backbone NH signal (detectable shortly after exchange into D_2O, but not two hours later) are indicated with a turquoise circle; those with a very slowly exchanging backbone NH signal (still detectable after 48 hours) are indicated with a dark blue circle. (For interpretation of the references to colour in this figure legend, the reader is referred to the web version of this article.)

Table 2
Structural statistics for the 20 best NMR structures of Arc-Aβ1–40(E22G) in a solution of H_2O + D_2O with SDS micelles.

Distance restraints used for structure calculation	Total
Interproton restraints	488
Intraresidue	296
Sequential ($\|i-j\| = 1$)	150
Medium-range ($1 < \|i-j\| \leqslant 4$)	42
Long-range ($\|i-j\| > 4$)	0

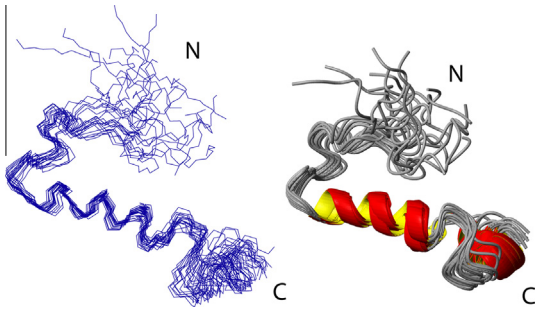

Fig. 3. The superposition of 20 minimized structures for the Arc-Aβ1–40(E22G) in a solution of H_2O + D_2O with SDS micelles. The best agreement is reached for residues L17-N27, RMSD backbone = 0.37 ± 0.17 Å and for residues L34-G38, RMSD backbone = 0.09 ± 0.04 Å.

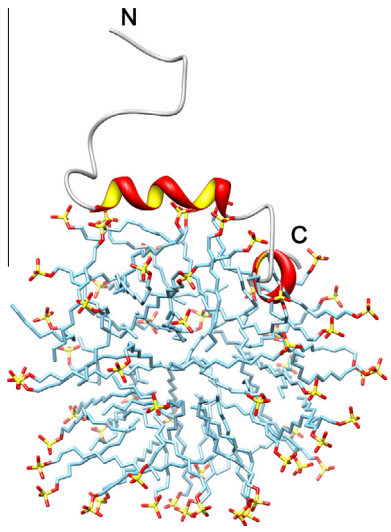

Fig. 4. Proposed structure for Arc-Aβ1–40(E22G) bound to a SDS micelle.

those of Val12, His13, Leu17, Val18, Phe20, Ala21, Val24 and Lys28, whereas the corresponding side chains for the Arctic variant are those of Val12, His13, Gln15, Leu17, Val18, Phe19, Phe20, Ala21, Val24 and Lys28. This difference suggests that the Arc-Aβ1–40 peptide fragment is immersed more deeply in the SDS micelle than the native Aβ1–40 peptide.

A study performed with full-length peptides by Grant et al. [73] showed that the Arctic mutation significantly destabilized the turn structure in the central folding region A21–A30. In the intramolecular contact map corresponding to the Arctic mutation, decreased numbers of contacts were observed in the central folding region of Aβ1–40 and Aβ1–42. Probably as a result of these changes, the fibrillogenic properties of Aβ variants with different lengths were found to have changed [13,18,23,74]. Finally, Arc-Aβ1–40 fibrils exhibit a variety of distinct morphologies, significantly different from those of the wild type [28].

Generally, we observed differences in the structures of wt-Aβ1–40 and the Arc-Aβ1–40 mutant in an SDS environment and showed that the Arctic mutant of Aβ1–40 interacts with the surface of SDS micelles mainly through its Leu17–Asn27 3_{10}-helical region, while the Ile31–Val40 region is buried in the hydrophobic interior of the micelle. In contrast, the wild-type Aβ1–40 interacts with SDS micelles through the Lys16–Asp23 α-helical region and the Gly29–Met35 region. Both the wild-type and the mutant peptide interactions with SDS micelles are hydrophobic in nature. Aβ can presumably form pores in membranes, and cause changes in neuronal and endothelial cell membrane permeability. In addition, Aβ containing "Arctic" mutations have been found to be more neurotoxic and aggregate more readily than wild-type Aβ peptides. Here, we propose that extension of the helical structure of Leu17–Asn27 in the Arctic variant and the high aliphaticity (neutrality) of C-terminal region is in agreement with the idea that the formation of ion-permeable pores by Arctic Aβ oligomers may be a possible mechanism of neuronal toxicity independent of oxidative damage and lipid peroxidation.

Early isothermal calorimetry studies by Seelig's group [75] indicated the electrostatic nature of an Aβ1–40-membrane association, while our data demonstrated that binding of both the wild-type and the Arctic mutation Aβ peptides to SDS micelles are predominantly hydrophobic in nature. This may be explained by the electrostatic mechanism in the initial peptide-SDS interaction step and by hydrophobic binding in the final step.

Conclusion

In this article, we report the conformation of the "Arctic" mutant of Aβ1–40 Alzheimer's amyloid peptide in sodium dodecyl sulfate micelle solutions as studied by 2D NMR spectroscopy. We demonstrate that the Arctic mutation of Aβ1–40 interacts with

the surface of SDS micelles mainly through the Leu17–Asn27 3_{10}-helical region and the Ile31–Val40 region is buried in the hydrophobic interior of the micelle, in contrast to the wild-type Aβ1–40, which interacts with SDS micelles through the Lys16–Asp23 α-helical region and the Gly29–Met35 region.

These observations clearly show that both the peptide conformation and peptide-to-SDS binding properties are very sensitive to single amino acid substitutions. Single amino acid substitutions may result in a change in the rate of fibrillation, reflected as pathogenicity differences of Aβ variants related to AD. We suggest that the importance of hydrophobic interactions of both the wild-type and the "Arctic" mutant peptides with SDS micelles may, in principle, be generalized to biomembranes, where zwitterionic lipids are dominating and the electrostatic interaction plays less significant role. However, this hypothesis requires more experimental studies, which are currently on the way in our laboratory.

Acknowledgements

The work is performed accordingly to the Russian Government Program of Competitive Growth of Kazan Federal University and by the subsidy allocated to Kazan Federal University for the state assignment in the sphere of scientific activities and also supported by Russian Foundation for Basic Research (Grant 14-04-31029 mol_a).

A.V.F and O.N.A are grateful to the Foundation in memory of J.C and Seth M. Kempe and the Swedish Alzheimer's fund for grants from which chemicals and equipment for the peptide synthesis and purification was purchased. We also acknowledge Dr. S. Afonin for electrospray mass-spectrometry analysis of peptides.

References

[1] D.M. Walsh, D.M. Hartley, Y. Kusumoto, Y. Fezoui, M.M. Condron, A. Lomakin, G.B. Benedek, D.J. Selkoe, D.B. Teplow, J. Biol. Chem. 274 (1999) 25945.
[2] J.C. Rochet, P.T. Lansbury, Curr. Opin. Struct. Biol. 10 (2000) 60.
[3] M. Bucciantini, E. Giannoni, F. Chiti, F. Baroni, L. Formigli, J.S. Zurdo, N. Taddei, G. Ramponi, C.M. Dobson, M. Stefani, Nature 416 (2002) 507.
[4] C.G. Glabe, Neurobiol. Aging 27 (2006) 570.
[5] W.L. Klein, W.B. Stine, D.B. Teplow, Neurobiol. Aging 25 (2004) 569.
[6] C. Haass, D.J. Selkoe, Nat. Rev. Mol. Cell. Biol. 8 (2007) 101.
[7] R. Kayed, E. Head, J.L. Thompson, T.M. McIntire, S.C. Milton, C.W. Cotman, C.G. Glabe, Science 300 (2003) 486.
[8] E.M. Snyder, Y. Nong, C.G. Almeida, S. Paul, T. Moran, E.Y. Choi, A.C. Nairn, M.W. Salter, P.J. Lombroso, G.K. Gouras, P. Greengard, Nat. Neurosci. 8 (2005) 1051.
[9] S.M. Butterfield, H.A. Lashuel, Angew. Chem. Int. Ed. 49 (2010) 5628.
[10] D.J. Selkoe, Physiol. Rev. 81 (2001) 741.
[11] J.J. Balbach, Y. Ishii, O.N. Antzutkin, R.D. Leapman, N.W. Rizzo, F. Dyda, J. Reed, R. Tycko, Biochemistry 39 (2000) 13748.
[12] O.N. Antzutkin, R.D. Leapman, J.J. Balbach, R. Tycko, Biochemistry 41 (2002) 15436.
[13] L. Miravalle, T. Tokuda, R. Chiarle, G. Giaccone, O. Bugiani, F. Tagliavini, B. Frangione, J. Ghiso, J. Biol. Chem. 275 (2000) 27110.
[14] J. Ghiso, B. Frangione, Adv. Drug. Deliver. Rev. 54 (2002) 1539.
[15] E. Levy, M.D. Carman, I.J. Fernandezmadrid, M.D. Power, I. Lieberburg, S.G. Vanduinen, G.T.A.M. Bots, W. Luyendijk, B. Frangione, Science 248 (1990) 1124.
[16] G. Rossi, G. Macchi, M. Porro, G. Giaccone, M. Bugiani, E. Scarpini, G. Scarlato, G.E. Molini, F. Sasanelli, O. Bugiani, F. Tagliavini, Neurology 50 (1998) 688.
[17] C. Nilsberth, A. Westlind-Danielsson, C.B. Eckman, M.M. Condron, K. Axelman, C. Forsell, C. Stenh, J. Luthman, D.B. Teplow, S.G. Younkin, J. Naslund, L. Lannfelt, Nat. Neurosci. 4 (2001) 887.
[18] A. Paivio, J. Jarvet, A. Graslund, L. Lannfelt, A. Westlind-Danielsson, J. Mol. Biol. 339 (2004) 145.
[19] A.S. Johansson, F. Berglind-Dehlin, G. Karlsson, K. Edwards, P. Gellerfors, L. Lannfelt, FEBS J. 273 (2006) 2618.
[20] L. Hendriks, C.M. Vanduijn, P. Cras, M. Cruts, W. Vanhul, F. Vanharskamp, A. Warren, M.G. Mcinnis, S.E. Antonarakis, J.J. Martin, A. Hofman, C. Vanbroeckhoven, Nat. Genet. 1 (1992) 218.
[21] T.J. Grabowski, H.S. Cho, J.P.G. Vonsattel, G.W. Rebeck, S.M. Greenberg, Ann. Neurol. 49 (2001) 697.
[22] H. Takuma, R. Teraoka, H. Mori, T. Tomiyama, Neuroreport 19 (2008) 615.
[23] W.E. Van Nostrand, J.P. Melchor, H.S. Cho, S.M. Greenberg, G.W. Rebeck, J. Biol. Chem. 276 (2001) 32860.
[24] A. Miravalle, K.L. Roos, Arch. Neurol. – Chicago 60 (2003) 925.
[25] H. Basun, N. Bogdanovic, M. Ingelsson, O. Almkvist, J. Naslund, K. Axelman, T.D. Bird, D. Nochlin, G.D. Schellenberg, L.O. Wahlund, L. Lannfelt, Arch. Neurol. – Chicago 65 (2008) 499.
[26] K.N. Dahlgren, A.M. Manelli, W.B. Stine, L.K. Baker, G.A. Krafft, M.J. LaDu, J. Biol. Chem. 277 (2002) 32046.
[27] H.A. Lashuel, D. Hartley, B.M. Petre, T. Walz, P.T. Lansbury, Nature 418 (2002) 291.
[28] N. Norlin, M. Hellberg, A. Filippov, A.A. Sousa, G. Grobner, R.D. Leapman, N. Almqvist, O.N. Antzutkin, J. Struct. Biol. 180 (2012) 174.
[29] I.H. Cheng, J. Palop, N. Bien-Ly, F.R. Yan, L. Mucke, Neurobiol. Aging 25 (2004) S256.
[30] H. Englund, D. Sehlin, A.S. Johansson, L.N.G. Nilsson, P. Gellerfors, S. Paulie, L. Lannfelt, F.E. Pettersson, J. Neurochem. 103 (2007) 334.
[31] J. Kyte, R.F. Doolittle, J. Mol. Biol. 157 (1982) 105.
[32] R. Riek, P. Guntert, H. Dobeli, B. Wipf, K. Wuthrich, Eur. J. Biochem. 268 (2001) 5930.
[33] L.M. Hou, H.Y. Shao, Y.B. Zhang, H. Li, N.K. Menon, E.B. Neuhaus, J.M. Brewer, I.J.L. Byeon, D.G. Ray, M.P. Vitek, T. Iwashita, R.A. Makula, A.B. Przybyla, M.G. Zagorski, J. Am. Chem. Soc. 126 (2004) 1992.
[34] N.G. Sgourakis, Y.L. Yan, S.A. McCallum, C.Y. Wang, A.E. Garcia, J. Mol. Biol. 368 (2007) 1448.
[35] D.J. Selkoe, J. Neurochem. 65 (1995) S136.
[36] D.J. Selkoe, Nature 375 (1995) 734.
[37] P.T. Lansbury, Proc. Nat. Acad. Sci. U.S.A. 96 (1999) 3342.
[38] D.M. Walsh, I. Klyubin, J.V. Fadeeva, W.K. Cullen, R. Anwyl, M.S. Wolfe, M.J. Rowan, D.J. Selkoe, Nature 416 (2002) 535.
[39] A.T. Petkova, R.D. Leapman, Z.H. Guo, W.M. Yau, M.P. Mattson, R. Tycko, Science 307 (2005) 262.
[40] R. Lal, H. Lin, A.P. Quist, BBA-Biomembranes 1768 (2007) 1966.
[41] S. Chimon, M.A. Shaibat, C.R. Jones, D.C. Calero, B. Aizezi, Y. Ishii, Nat. Struct. Mol. Biol. 14 (2007) 1157.
[42] L. Mäler, Mol. Membr. Biol. 29 (2012) 155.
[43] N.E. Gabriel, M.F. Roberts, Biophys. J. 45 (1984) A41.
[44] M.J. Hope, M.B. Bally, L.D. Mayer, A.S. Janoff, P.R. Cullis, Chem. Phys. Lipids 40 (1986) 89.
[45] L.D. Mayer, M.J. Hope, P.R. Cullis, Biochim. Biophys. Acta 858 (1986) 161.
[46] R.R. Vold, R.S. Prosser, A.J. Deese, J. Biomol. NMR 9 (1997) 329.
[47] C.R. Sanders, R.S. Prosser, Struct. Fold. Dis. 6 (1998) 1227.
[48] P. Damberg, J. Jarvet, A. Gräslund, Nucl. Magn. Reson. Biol. Macromol. B 339 (2001) 271.
[49] D.E. Warschawski, A.A. Arnold, M. Beaugrand, A. Gravel, E. Chartrand, I. Marcotte, BBA-Biomembranes 1808 (2011) 1957.
[50] J. Jarvet, J. Danielsson, P. Damberg, M. Oleszczuk, A. Gräslund, J. Biomol. Nucl. Magn. Reson. 39 (2007) 63.
[51] K.S. Usachev, S.V. Efimov, A.R. Yulmetov, A.V. Filippov, O.N. Antzutkin, S. Afonin, V.V. Klochkov, Magn. Reson. Chem. 50 (2012) 784.
[52] K.S. Usachev, A.V. Filippov, O.N. Antzutkin, V.V. Klochkov, Eur. Biophys. J. 42 (2013) 803.
[53] D.S. Blochin, O.V. Aganova, A.R. Yulmetov, A.V. Filippov, B.I. Gizatullin, S. Afonin, O.N. Antzutkin, V.V. Klochkov, J. Mol. Struct. 1033 (2013) 59.
[54] D.S. Blokhin, A.V. Filippov, O.N. Antzutkin, F.Kh. Karataeva, V.V. Klochkov, J. Mol. Struct. 1070 (2014) 38.
[55] A. Rauk, Dalton Trans. (2008) 1273.
[56] M. Coles, W. Bicknell, A.A. Watson, D.P. Fairlie, D.J. Craik, Biochemistry 37 (1998) 11064.
[57] D.S. Blokhin, S.V. Efimov, A.V. Klochkov, A.R. Yulmetov, A.V. Filippov, O.N. Antzutkin, A.V. Aganov, V.V. Klochkov, Appl. Magn. Reson. 41 (2011) 267.
[58] F. Delaglio, S. Grzesiek, G.W. Vuister, G. Zhu, J. Pfeifer, A. Bax, J. Biomol. NMR 6 (1995) 277.
[59] T.D. Goddard, D.G. Kneller, SPARKY 3, University of California, San Francisco.
[60] C.D. Schwieters, J.J. Kuszewski, N. Tjandra, G.M. Clore, J. Magn. Reson. 160 (2003) 65.
[61] R. Koradi, M. Billeter, K. Wuthrich, J. Mol. Graphics 14 (1996) 51.
[62] E.F. Pettersen, T.D. Goddard, C.C. Huang, G.S. Couch, D.M. Greenblatt, E.C. Meng, T.E. Ferrin, J. Comput. Chem. 25 (2004) 1605.
[63] K.S. Usachev, A.V. Filippov, E.A. Filippova, O.N. Antzutkin, V.V. Klochkov, J. Mol. Struct. 1049 (2013) 436.
[64] T. Kohno, K. Kobayashi, T. Maeda, K. Sato, A. Takashima, Biochemistry 35 (1996) 16094.
[65] T.G. Fletcher, D.A. Keire, Protein Sci. 6 (1997) 666.
[66] K.J. Marcinowski, H. Shao, E.L. Clancy, M.G. Zagorski, J. Am. Chem. Soc. 120 (1998) 11082.
[67] H.Y. Shao, S.C. Jao, K. Ma, M.G. Zagorski, J. Mol. Biol. 285 (1999) 755.
[68] P.K. Mandal, J.W. Pettegrew, Neurochem. Res. 29 (2004) 2267.
[69] J. Danielsson, J. Jarvet, P. Damberg, A. Gräslund, FEBS J. 272 (2005) 3938.
[70] S. Rodziewicz-Motowidlo, P. Czaplewska, E. Sikorska, M. Spodzieja, A.S. Kolodziejczyk, J. Struct. Biol. 164 (2008) 199.
[71] S. Vivekanandan, J.R. Brender, S.Y. Lee, A. Ramamoorthy, Biochem. Biophys. Res. Commun. 411 (2011) 312.
[72] M.G. Krone, A. Baumketner, S.L. Bernstein, T. Wyttenbach, N.D. Lazo, D.B. Teplow, M.T. Bowers, J.E. Shea, J. Mol. Biol. 381 (2008) 221.
[73] M.A. Grant, N.D. Lazo, A. Lomakin, M.M. Condron, H. Arai, G. Yamin, A.C. Rigby, D.B. Teplow, Proc. Nat. Acad. Sci. U.S.A. 104 (2007) 16522.
[74] K. Murakami, K. Irie, A. Morimoto, H. Ohigashi, M. Shindo, M. Nagao, T. Shimizu, T. Shirasawa, J. Biol. Chem. 278 (2003) 46179.
[75] E. Terzi, G. Holzemann, J. Seelig, J. Mol. Biol. 252 (1995) 633.